Closed-Form Waveform Design for MIMO Radar Transmit Beampattern Synthesis via Integral Equality

YEZI MA (Student Member, IEEE), **PING WEI**, **HUAGUO ZHANG**, AND **YAN PAN**
School of Information and Communication Engineering, University of Electronic Science and Technology of China, Chengdu 611731, China

Corresponding authors: Yezi Ma (yezi_ma@163.com) and Ping Wei (pwei@uestc.edu.cn)

ABSTRACT Recently, due to the adequate use of waveform diversity, MIMO technology has been widely adopted, resulting in the waveform design for MIMO radar beampattern synthesis becoming a hot issue. However, most previous works regarding this problem optimize the waveform by introducing the global mean squared error (MSE) as the cost function, this requires large computation in applications. Different from these works, we adopt the idea from the shaped beampattern synthesis problem of 2-D array in this paper, that is, to form a flat-top beampattern in the desired area with small ripple. By considering the physical meaning of the flat-top beampattern from scratch, the MIMO waveform design problem is turned to designing the waveforms that make its beampattern integral (i.e. the energy transmitted by array) equal in the desired area. Subsequently, we put forth a closed-form method and give its mathematical proof. Numerical simulations and comparisons to known MIMO radar waveform design methods are provided to verify its effectiveness and outperformance.

INDEX TERMS MIMO radar, waveform design, beampattern synthesis, closed-form method.

I. INTRODUCTION

In the past decade, multiple-input multiple-output (MIMO) technology has attracted widespread attention and been widely used in the fields of communication [1], [2], beamforming technique [3], [4], source localization [5]–[7] and target tracking [8]. MIMO has higher degree of freedom (DoF) than phased array due to its adequate use of waveform diversity [9], [10]. According to the antenna distribution, MIMO array can be classified into distributed MIMO and colocated MIMO. In MIMO system, each antenna transmits independent waveform to obtain higher resolution and larger array aperture, and this waveform can be designed to meet different requirements.

In MIMO communication, much attention is focused on the orthogonality of waveform to improve the communication quality [11], [12]. However, in MIMO radar, people are more concerned about how to design its waveform to take full advantage of the increased DoF of MIMO.

The associate editor coordinating the review of this manuscript and approving it for publication was Kai Lu.

Current research regarding the MIMO radar can be divided into two main categories: designing both transmit waveform and receiving filter; designing the transmit waveform only. The former one jointly designs the transmit waveform and the receiving filter to maximize the output signal-to-interference-plus-noise ratio (SINR) [13]–[22]. Specifically, for colocated MIMO radar, the transmit waveforms are designed to improve the SINR performance in the presence of signal clutter in signal [13]–[20]. For distributed MIMO radar, the transmit waveforms are designed by maximizing the mutual information (MI) between the receiving echoes and the target response [21], [22]. The latter category only designs the transmit waveform to flexibly control the distribution of the array transmit energy in space: that is the MIMO radar transmit beampattern synthesis problem [23], [24]. Recently, MIMO waveform design for its transmit beampattern matching is a hot issue in MIMO research and also the focus of this paper [25], [26].

In the latest works about MIMO beampattern matching problem, there are two types of methods: two-steps and one-step methods. The two-steps methods firstly design the

waveform covariance matrix R that matches the desired beampattern [27], [28]. However, it is difficult to directly obtain the waveform matrix S from its covariance matrix R. Calculating S from R requires special relaxation processing such as Semidefinite Quadratic Programming (SQP) and Cyclic Algorithm (CA) [9]. To avoid the relaxation processing, the one-step approaches such as AMDD [23] and DFT-based method [24] design the waveform S directly. However, all these methods, including the two-steps and the one-step methods, introduce certain optimizing strategies to design the waveform, requiring complicated calculations. On the contrary, the DFT-based method is not the case: it is a closed-form method. The DFT-based method can design the waveform that produces the beampattern matching the desired beampattern with low computational complexity. Nonetheless, the resolution of the DFT method is poor when the number of array element is small. In practice, increasing the number of array elements is usually inconvenient, indicating the limitation of the DFT-based method. In addition, in order to evaluate the performance of the designed waveforms, all these works use the global Mean-Squared Error (MSE) in the whole spatial domain as the optimized cost function and the performance evaluation criteria, leading to the fact that the designed waveforms may not have the best performance in the desired region. In engineering, for the problem of beampattern synthesis, more attention is focused on how to transmit energy to the desired area accurately.

Fundamentally, the increased DoF in MIMO radar comes from its time-varying waveform. In other words, MIMO radar adopts the strategy that takes time for space, and the MIMO array can be seen as a 2-D array with time-invariant parameters [29]. Thus, the shaped beampattern synthesis with 2-D time-invariant array (also a hot topic) is a similar problem to the MIMO radar beampattern synthesis. In the problem of shaped beampattern synthesis with time-invariant parameters, accurately transmitting the array energy to certain desired areas means forming flat-top beampatterns with smallest local MSE in the desired areas [30], [31]. However, this problem usually requires lots of optimizations as well [32]–[35]. Inspired by the shaped beampattern synthesis, unlike the previous work considering global MSE, we adopt the evaluation criterion of shaped beampattern synthesis [30], i.e., the local MSE in the desired region in this paper. Specifically, by designing the waveform directly, the MIMO beampattern is determined to match our desired beampattern as close as possible in the desired region [36]. By doing so, the problem turns to synthesizing a flat-top beampattern with small ripple in the desired region.

From the physical essence, a flat-top beampattern in the desired region means the energy transmitted by MIMO array is equal everywhere within the desired region [37], [38]. In fact, the transmit energy is the integral of transmit beampattern. However, because the beampattern expression does not have an analytic form, this integral is difficult to calculate directly.
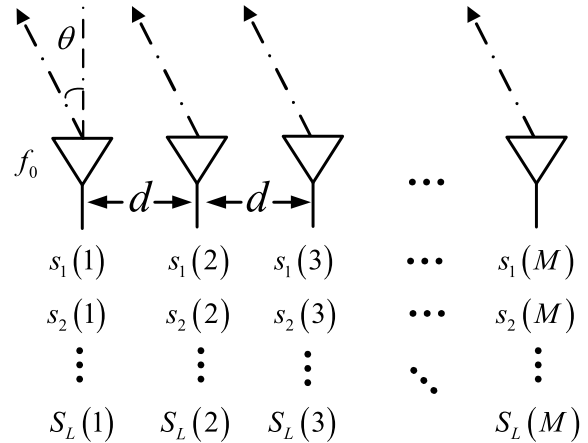

FIGURE 1. Structure of MIMO radar and illustration of MIMO waveform.

In this paper, we put forth a closed-form method that directly designs the MIMO waveform without optimizing. Our method first designs the phase excitation of waveform to make the beampattern expression analytical. Subsequently, we introduce a Taylor approximation to simplify the beampattern integral and deduce the magnitude excitations of waveform that can ensure the beampattern integral (i.e. the energy transmitted by array) equal in the desired region. The mathematical proof and the simulations are provided to verify its effectiveness and show the outperformance of our method.

The remainder of this paper are organized as follows. Section II formulates the beampattern synthesis problem for MIMO radar. Our closed-form method and its mathematical proof are provided in section III. Numerical simulations and comparison to known MIMO radar waveform design are given in Section IV. Section V presents the conclusion. Some necessary mathematical proofs are given in Appendices A and B.

Notation: We use uppercase (lowercase) bold-face letters to denote matrices (column vectors). $(\cdot)^T$ and $(\cdot)^H$ represent the transpose and conjugate transpose, respectively. $\sup(\cdot)$ denotes the supremum.

II. BEAMPATTERN SYNTHESIS PROBLEM FOR MIMO RADAR

In this paper, we consider a colocated Uniform Linear Array (ULA) MIMO. It is composed of M transmitting elements with uniform half-wavelength spacing d, as shown in FIGURE 1. Different from the traditional phased array radar, the transmitting waveform of MIMO radar is time-varying. The baseband waveform transmitted by the m-th element in sample l with carrier frequency f_0 is

$$s_l(m) = \alpha_l(m) e^{j\varphi_l(m)}$$
$$\text{for } l = 1, 2, \cdots, L, \ m = 1, 2, \cdots, M; \quad (1)$$

where $\alpha_l(m)$ and $\varphi_l(m)$ are the magnitude and phase excitations, respectively. The entry in the l-th row and m-th column
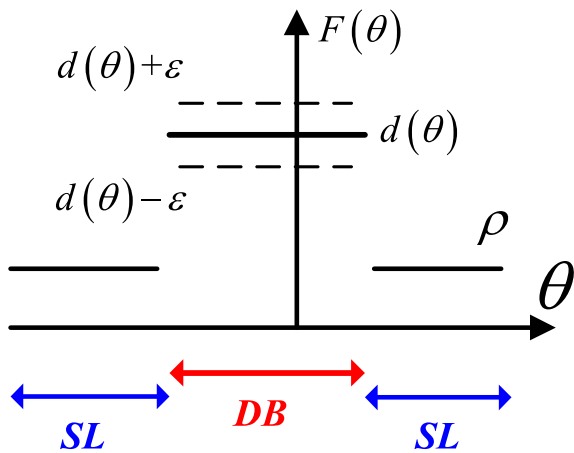
FIGURE 2. Illustration of transmit beampattern synthesis for MIMO radar.

FIGURE 3. Illustration of our method to form a flat-top beampattern: each intergral (i.e. transmit energy) on its mainlobe region Θ_l keeps equal.

of the waveform matrix $S \in \mathbb{C}^{L \times M}$ is $s_l(m)$, as shown in FIGURE 1.

All the waveforms in the waveform matrix S arrive at the far-field direction θ and coherently summate. As a result, the total energy radiated by the array seen at the direction θ is

$$F(\theta) = a^{\mathrm{H}}(\theta) R_{SS} a(\theta) = \sum_{l=1}^{L} f_l(\theta)$$

$$\text{with } f_l(\theta) = \left| \sum_{m=1}^{M} \alpha_l(m) e^{j\varphi_l(m)} e^{-jm2\pi f_0 d \sin\theta/c} \right|^2, \quad (2)$$

where

$$a(\theta) = \left[e^{-j\frac{2\pi}{c} f_0 d \sin\theta}, e^{-j2\frac{2\pi}{c} f_0 d \sin\theta}, \cdots, e^{-jM\frac{2\pi}{c} f_0 d \sin\theta} \right]^{\mathrm{T}}$$

is the steering vector, $R_{SS} = S^{\mathrm{H}} S / L$ the waveform covariance matrix, and $f_l(\theta)$ the radiating power of sample l.

For the MIMO radar beampattern synthesis problem, the core issue is to control the spatial distribution of transmit power to match our desired beampattern shape by designing the waveform matrix S. Different from the previous work designing S by optimizing global MSE, in this paper, as shown in the FIGURE 2, we introduce the 'distance' ε between the desired beampattern shaped $d(\theta)$ and the MIMO radar transmit beampattern $F(\theta)$ from the shaped beampattern synthesis problem [30]. In other words, we want to synthesize a flat-top beampattern with small ripple ε that leads to minimum local MSE in desired region. Then the synthesis problem can be written as

$$\min_{S} \varepsilon$$

$$s.t. \begin{cases} \sup |F(\theta) - d(\theta)| \leq \varepsilon, & \theta \in DB \\ |F(\theta)| \leq \rho, & \theta \in SL \end{cases} \quad (3)$$

where DB and SL are the Desired Beam region and the SideLobe region respectively. The sidelobes are kept

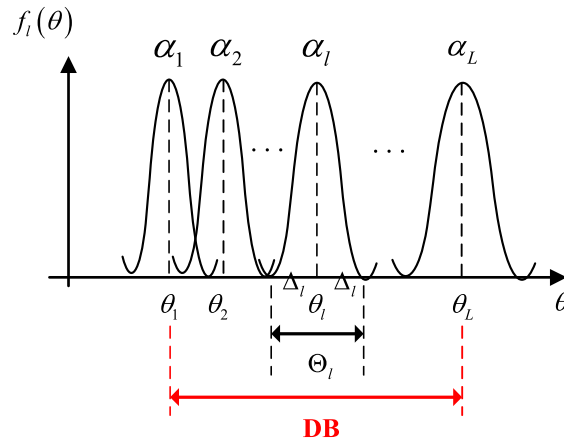below ρ, where the ρ indicates the overall sidelobe level. FIGURE 2 provides the graphic illustration.

This non-convex problem with multiple parameters is difficult to solve and may have more than one optimal solution. As mentioned in Section I, optimizing strategies such as CVX [30], CA [9] and ADMM [23] are used to solve this problem in many previous works. In this paper, for MIMO radar beampattern synthesis problem (3), we put forth a closed-form method with high accuracy.

III. OUR CLOSED-FORM METHOD AND ITS MATHEMATICAL PROOF

The focus of designing the waveform matrix S is the excitations. It is natural to think of the case where the conventional phased array is used at each sample, and the DB region is covered by their pointing angles, while the amplitude excitations keep the same. However, this setting cannot achieve optimal performance because the energy transmitting into certain region by phased arrays with different pointing angle is different.

Nonetheless, based on the above discussion, it is possible to simplify the problem. In our method, as shown in the FIGURE 3, the magnitude and phase excitations of m-th element in sample l are directly set as follows

$$\alpha_l(m) = \alpha_l = \sqrt{\cos\theta_l}, \quad \varphi_l(m) = m2\pi f_0 d \sin\theta_l / c, \quad (4)$$

where θ_l is a given angle and they cover the DB region. We still choose the phase excitations from the phased array as the phase excitations of our method, resulting in the array radiating power $f_l(\theta)$ having a closed-form expression. In this way, the problem of designing all excitations can be simplified into only designing the amplitude excitations. It is noted that the waveforms are costant-modulus across the array only in sample l. It can be achieved by the power divider in engineering. Furthermore, since all the excitations in (4) are only related to θ_l and they are given directly, our method has another advantage that each waveform is chosen from a

finite alphabet, which decreases the physical implementation complexity.

Taking (4) into (2) yields

$$
\begin{aligned}
f_l(\theta) &= \left| \sum_{m=1}^{M} \alpha_l(m) \, e^{j\varphi_l(m)} e^{-jm2\pi f_0 d \sin\theta/c} \right|^2 \\
&= \left| \alpha_l \frac{\sin\left(\frac{M\pi}{2}(\sin\theta - \sin\theta_l)\right)}{\sin\left(\frac{\pi}{2}(\sin\theta - \sin\theta_l)\right)} \right|^2,
\end{aligned} \tag{5}
$$

which makes $f_l(\theta)$ having a closed-form expression as mentioned above. However, due to that the relationship between θ and $f_l(\theta)$ is still not a combination of basic functions, equation (5) requires further simplification. As shown in FIGURE 3, in the mainlobe region Θ_l of θ_l, θ is close to θ_l, hence the following two approximations can be introduced to simplify the equation (5)

$$
\sin\left(\pi(\sin\theta - \sin\theta_l)/2\right) \approx \pi(\sin\theta - \sin\theta_l)/2, \tag{6a}
$$
$$
\sin\theta - \sin\theta_l \approx \cos\theta_l(\theta - \theta_l). \tag{6b}
$$

The approximation (6a) comes from the equivalent infinitesimal of sine function and the derivation of (6b) can be seen in the APPENDIX A. Taking the approximations (6) to the equation (5), the equation (5) can be simplified as

$$
\begin{aligned}
f_l(\theta) &= \left| \alpha_l \frac{\sin\left(\frac{M\pi}{2}(\sin\theta - \sin\theta_l)\right)}{\sin\left(\frac{\pi}{2}(\sin\theta - \sin\theta_l)\right)} \right|^2 \\
&\approx \alpha_l{}^2 \left| \frac{\sin\left(\frac{M\pi}{2}(\sin\theta - \sin\theta_l)\right)}{\frac{\pi}{2}(\sin\theta - \sin\theta_l)} \right|^2 \\
&\approx \alpha_l{}^2 \left| \frac{\sin\left(\frac{M\pi}{2}\cos\theta_l(\theta - \theta_l)\right)}{\frac{\pi}{2}\cos\theta_l(\theta - \theta_l)} \right|^2.
\end{aligned} \tag{7}
$$

So far, equation (7) is approximated to the simplest and analytical form. The physical meaning of equation (7) is the array radiating power at direction θ in sample l, which is mainly focused near θ_l.

Back to the MIMO radar beampattern synthesis problem, the goal of problem (3) is synthesizing a flat-top beampattern with small ripple ε. Put differently, the array radiating energy on its mainbeam region $\Theta_l \in [\theta_l - \Delta_l, \theta_l + \Delta_l]$ is an integral

$$
\begin{aligned}
&\int_{\theta \in \Theta_l} f_l(\theta) d\theta \\
&= \int_{\theta \in \Theta_l} \alpha_l{}^2 \left| \frac{\sin\left(\frac{M\pi}{2}\cos\theta_l(\theta - \theta_l)\right)}{\frac{\pi}{2}\cos\theta_l(\theta - \theta_l)} \right|^2 d\theta,
\end{aligned} \tag{8}
$$

which should keep constant. This means that no matter how θ_l changes, the array radiating energy on its mainlobe region Θ_l remains unchanged by controlling the magnitude excitations α_l. By doing so, the flat-top beampattern synthesis problem can be transformed into finding the α_l that keeps the integral in (8) equal. FIGURE 3 provides the detailed graphic illustration.

Unfortunately, the integral in (8) is a transcendental integral that does not have a solution with

mathematically-closed form. In this paper, in order to analytically calculate the integral (8), we introduce the Taylor approximation as

$$
\begin{aligned}
&\left(\frac{\sin\left(\frac{M\pi}{2}\cos\theta_l(\theta - \theta_l)\right)}{\frac{\pi}{2}\cos\theta_l(\theta - \theta_l)} \right)^2 \\
&\approx M^2 \left(1 - \frac{1}{3}\left(\frac{M\pi}{2}\cos\theta_l(\theta - \theta_l)\right)^2 \right).
\end{aligned} \tag{9}
$$

The detailed Taylor expansion for equation (9) is provided in APPENDIX B.

The integral interval Θ_l of the integral (8) is the mainlobe region of θ_l and its width Δ_l can be obtained from equation (9)

$$
1 - \frac{1}{3}\left(\cos\theta_l \frac{M\pi}{2}(\theta - \theta_l)\right)^2 = 0
$$
$$
\Rightarrow (\theta - \theta_l) = \Delta_l = \frac{2\sqrt{3}}{M\pi\cos\theta_l}. \tag{10}
$$

Taking (9) and the integral interval (10) into the integral (8) yields

$$
\begin{aligned}
&\int_{\theta \in \Theta_l} f_l(\theta) d\theta \\
&\approx \alpha_l{}^2 M^2 \int_{\theta_l - \Delta_l}^{\theta_l + \Delta_l} \left[1 - \frac{1}{3}\left(\cos\theta_l \frac{M\pi}{2}(\theta - \theta_l)\right)^2 \right] d\theta \\
&= \alpha_l{}^2 M^2 \int_{-\Delta_l}^{\Delta_l} \left[1 - \frac{M^2\pi^2}{12}\cos^2\theta_l(\theta - \theta_l)^2 \right] d(\theta - \theta_l) \\
&= \alpha_l{}^2 M^2 \left(2\Delta_l - \frac{M^2\pi^2}{18}\cos^2\theta_l \cdot \Delta_l{}^3 \right) \\
&= \alpha_l{}^2 M^2 \left[2\frac{2\sqrt{3}}{M\pi\cos\theta_l} - \frac{M^2\pi^2}{18}\cos^2\theta_l \cdot \left(\frac{2\sqrt{3}}{M\pi\cos\theta_l}\right)^3 \right] \\
&= \frac{\alpha_l{}^2}{\cos\theta_l} \frac{8\sqrt{3}M}{3\pi}.
\end{aligned} \tag{11}
$$

Thus, equation (11) provides the mathematical proof to confirm that the magnitude excitations $\alpha_l = \sqrt{\cos\theta_l}$ of our method (4) can ensure that the array radiating energy on spatial region Θ_l remains equal. So far, we solve the problem (3) analytically.

IV. SIMULATIONS

In the simulation section, we assume a ULA composed of $M = 10$ identical transmitting elements with uniform half-wavelength spacing $d = c/(2f_0)$, where the carrier frequency $f_0 = 1GHz$. For comparison, the simulation setting is exactly the same as [23], in which the sample number is $L = 32$ and the simulation range of angle dimension is $[-90°, 90°]$ with spacing $1°$.

With this setup, the simulations and comparisons to known MIMO radar waveform design methods such as CA [9], ADMM [23] and DFT-based [24] are provided to show the performances. It is worth to point out that we compare our
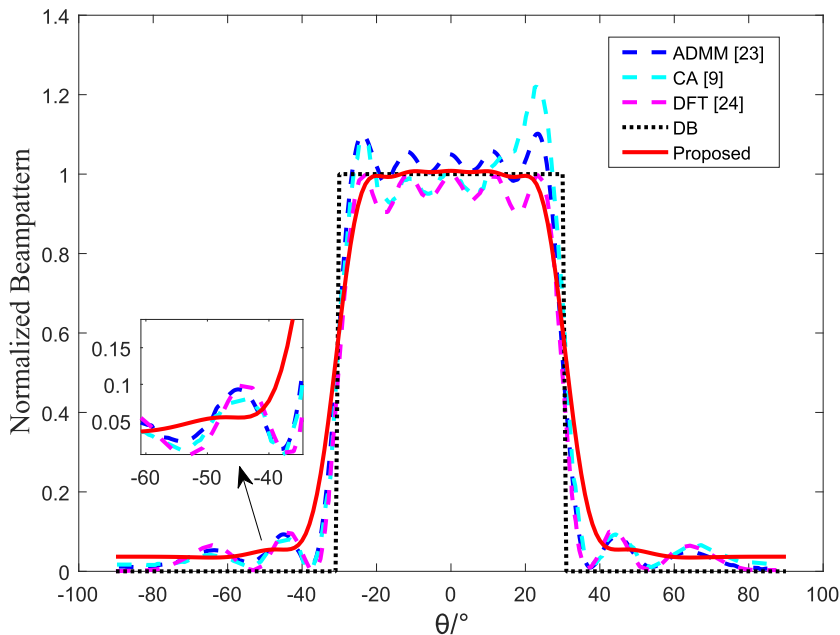
FIGURE 4. The simulation result of Example A: the case of the DB has one mainlobe beam.

method with the optimizing methods [9], [23] and the analytical method [24].

As what discussed in previous sections, we adopt the local MSEs in the desired region from the shaped beampattern synthesis problem as the criterion to evaluate the performances. The local MSE in DB region is defined as

$$\text{MSE}_{Local} = \frac{1}{K} \sum_{k=1}^{K} \left(\tilde{F}(\theta_k) - d(\theta_k) \right)^2, \quad \theta_k \in DB; \quad (12)$$

where $\tilde{F}(\theta)$ is the normalized transmit beampattern. In this section, as same as [23], we also consider two classical cases: one mainlobe beam and multiple mainlobe beams in DB region. Meanwhile, the overall sidelobe performance in SL region and the computational complexities of each method are also provided.

A. ONE MAINLOBE BEAM

In this example, the one mainlobe beampattern is considered. The DB region is $[-30°, 30°]$ with the desired beampattern

$$d(\theta) = \begin{cases} 1, & \theta \in [-30°, 30°] \\ 0, & else. \end{cases} \quad (13)$$

The L pointing angles $\theta_l = \theta_1, \theta_2, \ldots, \theta_L$ related to phase excitations are uniformly distributed on the DB. The L magnitude excitations $\alpha_l = \alpha_1, \alpha_2, \ldots, \alpha_L$ are set as our method (4), that is $\alpha_l = \sqrt{\cos \theta_l}$. The simulation results are presented in FIGURE 4.

Whether compared with the optimization method [9], [23] or the analytical method [24], the beampattern of our proposed method with ripple $\varepsilon = 0.008$ is the closest one to the desired flat-top beampattern in the DB region. Moreover,

the overall sidelobe of the proposed method in SL region are the smallest one.

B. THREE MAINLOBES BEAM

In this example, we provide a case in which DB has multibeams. The desired beampattern has three mainlobes:

$$d(\theta) = \begin{cases} 1, & \theta \in [-50°, -30°] \cup [-10°, 10°] \cup [30°, 50°] \\ 0, & else. \end{cases}$$

$$(14)$$

The center points of DB in this example are $-40°$, $0°$ and $40°$ respectively, each mainlobe has a width $20°$. As same as Example A, the $L = 32$ pointing angles $\theta_l = \theta_1, \theta_2, \ldots, \theta_L$ are uniformly distributed on the DB either. Because 32 is not a multiple of 3, for the three mainlobes in this case, 11, 10 and 11 samples are allocated for each one. The magnitude excitations are also $\alpha_l = \sqrt{\cos \theta_l}$, as equation (4). The simulation result is shown in FIGURE 5.

FIGURE 5 demonstrates that in the case of DB has multiple mainlobes, the proposed method is also the closest one to the desired beampattern. Its overall sidelobes performance is better than the DFT-based method, but slightly inferior to the optimization method. That is consistent with the law of conservation of energy, because the proposed method improve the local MSE performance greatly in this case. Moreover, the two sides are slightly higher than the middle one, because there is one more sample on each side as allocated above.

C. DISCUSSION

FIGURE 4 and FIGURE 5 show that the methods introducing optimizing strategies such as CA [9] and ADMM [23]
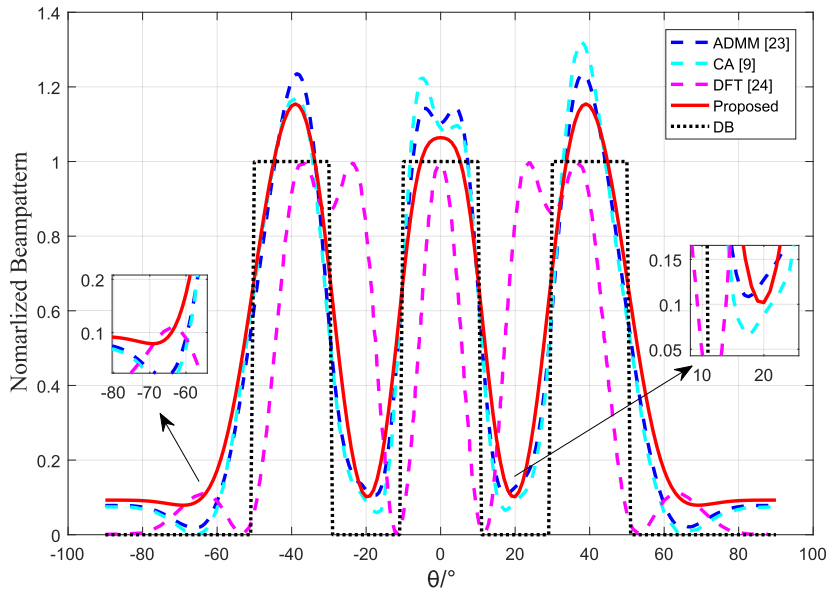
FIGURE 5. The simulation result of Example B: the case of the DB has three mainlobe beams.

TABLE 1. Performance comparison and computational complexity of each method.

Algorithm	Computational Complexity	Local MSE in DB region		Overall Sidelobe in SL region	
		One Mainbeam	Three Mainbeams	One Mainbeam	Three Mainbeams
CA [9]	$O(M^{3.5}N + M^2L^3)$	0.0115	0.0364	0.08	0.074
ADMM [23]	$O(M^3L)$	0.0119	0.0373	0.093	0.075
DFT [24]	$O(Mlog(M))$	0.0158	0.2358	0.1	0.11
Proposed	$O(1)$	0.0080	0.0222	0.055	0.093

have better performances than the closed-form one (i.e. the DFT-based method [24]) with the cost of higher computational complexity. However, high computational complexity has a limitation on the real-time implementation. Although the DFT-based method is also a closed-form approach, it cannot achieve good performance because the array element number is too small, and the DFT transform itself still requires calculation. Furthermore, the TABLE 1 demonstrates that the better the performance in DB region, the higher overall sidelobe in SL region. This is due to the law of energy conservation.

For the MIMO waveform design problem, regardless of whether the DB has one mainlobe or multiple mainlobes, our proposed method is the closest one to the desired flat-top beam in the DB. The local MSE in TABLE 1 also confirm the performance of our method. We achieve the flat-top beampattern by equalizing the array radiating energy on the desired spatial area.

Moreover, as can be seen from TABLE 1, our method not only has an improvement in the local MSE performance, but also minimizes the computational complexity. Meanwhile, its overall sidelobe performance remains below a low value. In fact, because our method is completely closed-form and all the excitations of the waveforms are designed directly as

equation (4), the computational complexity of the proposed method is $O(1)$.

In sum, in the MIMO waveform design for beampattern synthesis problem, our method can achieve the best performance with smallest computational complexity. As deduced above, this benefit comes from the fact that we consider the physical meaning of the flat-top beampattern from scratch and find the waveforms that equalize the beampattern integrals.

Despite this, as this paper considers the uniform array and instantaneously constant modulus for MIMO waveform design, we aim to design a more general waveform in the future publication.

V. CONCLUSION

In this paper, we put forth a closed-form method for MIMO radar transmit beampattern synthesis problem by reconsidering its physical meaning from scratch. Unlike previous work optimizing the waveform by introducing the global MSE as the cost function, we use the idea from shaped beampattern synthesis problem of 2-D array, which synthesis the beampattern with the smallest local MSE in the desired area. Therefore, designing the MIMO waveform for beampattern matching is turned to form a flat-top beampattern with small

ripple in the desired area. Subsequently, by discussing the physical essence of the flat-top beampattern, we deduce a method that can keep its beampattern integral (i.e. the energy transmitted by array) equal everywhere in the desired area, indicating a flat-top beampattern. The necessary mathematical proof is provided to demonstrate the validity of our method. Moreover, simulation results and comparisons to known MIMO radar waveform design methods show that our method outperforms in MIMO radar beampattern synthesis problem.

APPENDIX A
DERIVATION OF THE APPROXIMATION (6b)

In this section, we give a brief derivation of the approximation in equation (6b). As mentioned above, in the mainlobe region Θ_l of θ_l, θ is close to θ_l. The geometrical relationship can be written as

$$\theta = \theta_l - \Delta\theta, \tag{15}$$

where $\Delta\theta$ is a tiny angle difference. There is

$$
\begin{aligned}
\sin\theta &= \sin(\theta_l - \Delta\theta) \\
&= \sin\theta_l \cos\Delta\theta - \cos\theta_l \sin\Delta\theta \\
&\approx \sin\theta_l\left(1 - \frac{1}{2}\Delta\theta^2\right) - \cos\theta_l \Delta\theta \\
&= \sin\theta_l - \cos\theta_l(\theta_l - \theta) - \frac{1}{2}\Delta\theta^2 \sin\theta_l \\
&\approx \sin\theta_l - \cos\theta_l(\theta_l - \theta) \\
&\Rightarrow \sin\theta - \sin\theta_l = \cos\theta_l(\theta - \theta_l).
\end{aligned}
\tag{16}
$$

The first approximation in equation (16) comes from the Taylor approximation $\cos\Delta\theta \approx \left(1 - \Delta\theta^2/2\right)$ and $\sin\Delta\theta \approx \Delta\theta$. Moreover, the tiny $\Delta\theta$ leads to $\Delta\theta^2 \approx 0$, resulting the second approximation.

APPENDIX B
DERIVATION OF THE TAYLOR APPROXIMATION IN EQUATION (9)

This section provides the detailed Taylor approximating process in equation (9). The function is

$$f(\theta) = \left(\frac{\sin\left(\frac{M\pi}{2}\cos\theta_l(\theta - \theta_l)\right)}{\frac{\pi}{2}\cos\theta_l(\theta - \theta_l)}\right)^2, \tag{17}$$

The Second-Order Taylor approximation of the equation (17) in the point θ_l is

$$f(\theta) \approx f(\theta_l) + f^{(1)}(\theta_l)(\theta - \theta_l) + \frac{1}{2}f^{(2)}(\theta_l)(\theta - \theta_l)^2, \tag{18}$$

where the $f^{(n)}(\theta)$ denotes the n-order derivative of function $f(\theta)$ and they are

$$
\begin{aligned}
&f^{(1)}(\theta) \\
&= \frac{8\sin\left(\frac{M\pi\cos\theta_l(\theta_l - \theta)}{2}\right)^2}{\pi^2\cos^2\theta_l(\theta_l - \theta)^3} \\
&\quad - \frac{4M\cos\left(\frac{M\pi\cos\theta_l(\theta_l-\theta)}{2}\right)\sin\left(\frac{M\pi\cos\theta_l(\theta_l-\theta)}{2}\right)}{\pi\cos\theta_l(\theta_l-\theta)^2},
\end{aligned}
\tag{19a}
$$

$$
\begin{aligned}
&f^{(2)}(\theta) \\
&= \frac{2M^2\cos\left(\frac{M\pi\cos\theta_l(\theta_l-\theta)}{2}\right)^2}{(\theta_l - \theta)^2} \\
&\quad - \frac{2M^2\sin\left(\frac{M\pi\cos\theta_l(\theta_l-\theta)}{2}\right)^2}{(\theta_l - \theta)^2} \\
&\quad + \frac{24\sin\left(\frac{M\pi\cos\theta_l(\theta_l-\theta)}{2}\right)^2}{\pi^2\cos^2\theta_l(\theta_l-\theta)^4} \\
&\quad - \frac{16M\cos\left(\frac{M\pi\cos\theta_l(\theta_l-\theta)}{2}\right)\sin\left(\frac{M\pi\cos\theta_l(\theta_l-\theta)}{2}\right)}{\pi\cos\theta_l(\theta_l-\theta)^3}.
\end{aligned}
\tag{19b}
$$

Therefore, each coefficient of the Taylor approximation (18) can be obtained by calculating the limits below

$$f(\theta_l) = \lim_{\theta\to\theta_l}\left(\frac{\sin\left(\frac{M\pi}{2}(\theta - \theta_l)\cos\theta_l\right)}{\frac{\pi}{2}(\theta - \theta_l)\cos\theta_l}\right)^2 = M^2, \tag{20a}$$

$$f^{(1)}(\theta_l) = \lim_{\theta\to\theta_l} f^{(1)}(\theta) = 0, \tag{20b}$$

$$f^{(2)}(\theta_l) = \lim_{\theta\to\theta_l} f^{(2)}(\theta) = -\frac{M^4\pi^2\cos^2\theta_l}{6}. \tag{20c}$$

All the limits in equation (20) are '$0/0$'-style limitations that can be calculated by the L'Hospital's rule or the MATLAB function 'limit'. Taking theses coefficients in (20) back to the Taylor approximation (18) yields

$$
\begin{aligned}
f(\theta) &\approx f(\theta_l) + f^{(1)}(\theta_l)(\theta - \theta_l) + \frac{1}{2}f^{(2)}(\theta_l)(\theta - \theta_l)^2 \\
&= M^2 - \frac{1}{2}\frac{M^4\pi^2\cos^2\theta_l}{6}(\theta - \theta_l)^2 \\
&= M^2\left(1 - \frac{1}{3}\left(\frac{M\pi\cos\theta_l(\theta - \theta_l)}{2}\right)^2\right).
\end{aligned}
\tag{21}
$$

It is the approximation in equation (9).

REFERENCES

[1] A. Paulraj, D. Gore, R. U. Nabar, and H. Bolcskei, "An overview of MIMO communications–a key to gigabit wireless," *Proc. IEEE*, vol. 92, no. 2, pp. 198–218, Feb. 2004.

[2] R. Zhang and C. K. Ho, "MIMO broadcasting for simultaneous wireless information and power transfer," *IEEE Trans. Wireless Commun.*, vol. 12, no. 5, pp. 1989–2001, May 2013.

[3] S. Imani, M. Bolhasani, S. A. Ghorashi, and M. Rashid, "Waveform design in MIMO radar using radial point interpolation method," *IEEE Commun. Lett.*, vol. 22, no. 10, pp. 2076–2079, Oct. 2018.

[4] L. Guo, H. Deng, B. Himed, T. Ma, and Z. Geng, "Waveform optimization for transmit beamforming with MIMO radar antenna arrays," *IEEE Trans. Antennas Propag.*, vol. 63, no. 2, pp. 543–552, Feb. 2015.

[5] J. Xu, G. Liao, S. Zhu, L. Huang, and H. C. So, "Joint range and angle estimation using MIMO radar with frequency diverse array," *IEEE Trans. Signal Process.*, vol. 63, no. 13, pp. 3396–3410, Jul. 2015.

[6] D. E. Hack, L. K. Patton, B. Himed, and M. A. Saville, "Detection in passive MIMO radar networks," *IEEE Trans. Signal Process.*, vol. 62, no. 11, pp. 2999–3012, Jun. 2014.

[7] H. Yang, J. Chun, and D. Chae, "Hyperbolic localization in MIMO radar systems," *IEEE Antennas Wireless Propag. Lett.*, vol. 14, pp. 618–621, 2015.

[8] I. Bekkerman and J. Tabrikian, "Target detection and localization using MIMO radars and sonars," *IEEE Trans. Signal Process.*, vol. 54, no. 10, pp. 3873–3883, Oct. 2006.

[9] P. Stoica, J. Li, and X. Zhu, "Waveform synthesis for diversity-based transmit beampattern design," *IEEE Trans. Signal Process.*, vol. 56, no. 6, pp. 2593–2598, Jun. 2008.

[10] J. Li and P. Stoica, "MIMO radar with colocated antennas," *IEEE Signal Process. Mag.*, vol. 24, no. 5, pp. 106–114, Sep. 2007.

[11] U.-K. Kwon, D. Kim, and G.-H. Im, "Amplitude clipping and iterative reconstruction of MIMO-OFDM signals with optimum equalization," *IEEE Trans. Wireless Commun.*, vol. 8, no. 1, pp. 268–277, Jan. 2009.

[12] Z. Xiang, M. Tao, and X. Wang, "Massive MIMO multicasting in noncooperative cellular networks," *IEEE J. Sel. Areas Commun.*, vol. 32, no. 6, pp. 1180–1193, Jun. 2014.

[13] G. Cui, H. Li, and M. Rangaswamy, "MIMO radar waveform design with constant modulus and similarity constraints," *IEEE Trans. Signal Process.*, vol. 62, no. 2, pp. 343–353, Jan. 2014.

[14] O. Aldayel, V. Monga, and M. Rangaswamy, "Successive QCQP refinement for MIMO radar waveform design under practical constraints," *IEEE Trans. Signal Process.*, vol. 64, no. 14, pp. 3760–3774, Jul. 2016.

[15] B. Jiu, H. Liu, X. Wang, L. Zhang, Y. Wang, and B. Chen, "Knowledge-based spatial-temporal hierarchical MIMO radar waveform design method for target detection in heterogeneous clutter zone," *IEEE Trans. Signal Process.*, vol. 63, no. 3, pp. 543–554, Feb. 2015.

[16] S. Ahmed and M.-S. Alouini, "MIMO-radar waveform covariance matrix for high SINR and low side-lobe levels," *IEEE Trans. Signal Process.*, vol. 62, no. 8, pp. 2056–2065, Apr. 2014.

[17] S. Sen, "PAPR-constrained Pareto-optimal waveform design for OFDM-STAP radar," *IEEE Trans. Geosci. Remote Sens.*, vol. 52, no. 6, pp. 3658–3669, Jun. 2014.

[18] G. Cui, X. Yu, V. Carotenuto, and L. Kong, "Space-time transmit code and receive filter design for colocated MIMO radar," *IEEE Trans. Signal Process.*, vol. 65, no. 5, pp. 1116–1129, Mar. 2017.

[19] M. Bolhasani, E. Mehrshahi, and S. A. Ghorashi, "Waveform covariance matrix design for robust signal-dependent interference suppression in colocated MIMO radars," *Signal Process.*, vol. 152, pp. 311–319, Nov. 2018.

[20] M. Bolhasani, E. Mehrshahi, S. A. Ghorashi, and M. S. Alijani, "Constant envelope waveform design to increase range resolution and SINR in correlated MIMO radar," *Signal Process.*, vol. 163, pp. 59–65, Oct. 2019.

[21] Y. Chen, Y. Nijsure, C. Yuen, Y. H. Chew, Z. Ding, and S. Boussakta, "Adaptive distributed MIMO radar waveform optimization based on mutual information," *IEEE Trans. Aerosp. Electron. Syst.*, vol. 49, no. 2, pp. 1374–1385, Apr. 2013.

[22] Y. Yang and R. Blum, "MIMO radar waveform design based on mutual information and minimum mean-square error estimation," *IEEE Trans. Aerosp. Electron. Syst.*, vol. 43, no. 1, pp. 330–343, Jan. 2007.

[23] Z. Cheng, Z. He, S. Zhang, and J. Li, "Constant modulus waveform design for MIMO radar transmit beampattern," *IEEE Trans. Signal Process.*, vol. 65, no. 18, pp. 4912–4923, Sep. 2017.

[24] T. Bouchoucha, S. Ahmed, T. Al-Naffouri, and M.-S. Alouini, "DFT-based closed-form covariance matrix and direct waveforms design for MIMO radar to achieve desired beampatterns," *IEEE Trans. Signal Process.*, vol. 65, no. 8, pp. 2104–2113, Apr. 2017.

[25] Z. Cheng, Z. He, B. Liao, and M. Fang, "MIMO radar waveform design with PAPR and similarity constraints," *IEEE Trans. Signal Process.*, vol. 66, no. 4, pp. 968–981, Feb. 2018.

[26] Z. Cheng, C. Han, B. Liao, Z. He, and J. Li, "Communication-aware waveform design for MIMO radar with good transmit beampattern," *IEEE Trans. Signal Process.*, vol. 66, no. 21, pp. 5549–5562, Nov. 2018.

[27] M. Bolhasani, S. Imani, and S. A. Ghorashi, "A simple and fast method to generate transmit beampattern in MIMO radar," *Int. J. Innov. Res. Elect. Electron. Instrum. Control Eng.*, vol. 3, no. 8, pp. 77–82, Aug. 2015.

[28] M. Bolhasani, E. K. Ghafi, S. A. Ghorashi, and E. Mehrshahi, "Waveform covariance matrix design using Fourier series coefficients," *IET Signal Process.*, vol. 13, no. 5, pp. 562–567, Jul. 2019.

[29] P. Rocca, G. Oliveri, R. J. Mailloux, and A. Massa, "Unconventional phased array architectures and design methodologies—A review," *Proc. IEEE*, vol. 104, no. 3, pp. 544–560, Mar. 2016.

[30] B. Fuchs, A. Skrivervik, and J. R. Mosig, "Shaped beam synthesis of arrays via sequential convex optimizations," *IEEE Antennas Wireless Propag. Lett.*, vol. 12, pp. 1049–1052, 2013.

[31] J.-Y. Li, Y.-X. Qi, and S.-G. Zhou, "Shaped beam synthesis based on superposition principle and Taylor method," *IEEE Trans. Antennas Propag.*, vol. 65, no. 11, pp. 6157–6160, Nov. 2017.

[32] B. Fuchs, "Application of convex relaxation to array synthesis problems," *IEEE Trans. Antennas Propag.*, vol. 62, no. 2, pp. 634–640, Feb. 2014.

[33] B. Fuchs and S. Rondineau, "Array pattern synthesis with excitation control via norm minimization," *IEEE Trans. Antennas Propag.*, vol. 64, no. 10, pp. 4228–4234, Oct. 2016.

[34] B. Fuchs, "Shaped beam synthesis of arbitrary arrays via linear programming," *IEEE Antennas Wireless Propag. Lett.*, vol. 9, pp. 481–484, 2010.

[35] B. Fuchs, "Synthesis of sparse arrays with focused or shaped beampattern via sequential convex optimizations," *IEEE Trans. Antennas Propag.*, vol. 60, no. 7, pp. 3499–3503, Jul. 2012.

[36] Y. Ma, P. Wei, and H. Zhang, "General focusing beamformer for FDA: Mathematical model and resolution analysis," *IEEE Trans. Antennas Propag.*, vol. 67, no. 5, pp. 3089–3100, May 2019.

[37] X. Cai and W. Geyi, "An optimization method for the synthesis of flat-top radiation patterns in the Near- and far-field regions," *IEEE Trans. Antennas Propag.*, vol. 67, no. 2, pp. 980–987, Feb. 2019.

[38] A. Aghasi, H. Amindavar, E. L. Miller, and J. Rashed-Mohassel, "Flat-top footprint pattern synthesis through the design of arbitrary planar-shaped apertures," *IEEE Trans. Antennas Propag.*, vol. 58, no. 8, pp. 2539–2552, Aug. 2010.

YEZI MA (Student Member, IEEE) was born in Nanning, Guangxi, China. She received the B.S. degree in applied physics from the University of Electronic Science and Technology of China, Chengdu, China, in 2012, where she is currently pursuing the Ph.D. degree in signal and information processing, with a focus on array signal processing, frequency diverse array, and MIMO technique.

PING WEI received the B.S. and M.S. degrees in electronic engineering from the Beijing Institute of Technology, Beijing, China, in 1986 and 1989, respectively, and the Ph.D. degree in communication and electronic system from the University of Electronic Science and Technology of China (UESTC), Chengdu, China, in 1996. He is currently a Professor with the School of Information and Communication Engineering, UESTC. His current research interests include spectral analysis, array signal processing, electronic surveillance, and communication signal processing.

HUAGUO ZHANG received the Ph.D. degree in signal and information processing from the University of Electronic Science and Technology of China, Chengdu, China, in 2011. He is currently an Associate Professor with the School of Information and Communication Engineering, University of Electronic Science and Technology of China. His current research interests include noncooperative communication signal processing and array signal processing.

YAN PAN was born in Liuzhou, Guangxi, China. He received the B.Eng. degree in signal processing and instrumentation from Jilin University, Changchun, China, in 2018. He is currently pursuing the master's degree in electronics and communication engineering with the University of Electronic Science and Technology of China, Chengdu, China.

• • •